

# BTDAzo - a photoswitchable TRPC5 channel activator

Markus Müller,<sup>a</sup> Konstantin Niemeyer,<sup>b</sup> Nicole Urban,<sup>b</sup> Navin K. Ojha,<sup>c</sup> Frank Zufall,<sup>c</sup> Trese Leinders-Zufall,<sup>c</sup> Michael Schaefer,<sup>b</sup> Oliver Thorn-Seshold<sup>a\*</sup>

- [a] M. Müller, Dr. O. Thorn-Seshold  
Department of Pharmacy  
LMU Munich  
Butenandtstrasse 7, Munich 81377, Germany  
E-mail: oliver.thorn-seshold@cup.lmu.de
- [b] K. Niemeyer, N. Urban, Prof. Dr. M. Schaefer  
Rudolf-Boehm-Institute of Pharmacology and Toxicology  
Leipzig University  
Härtelstraße 16-18, 04107 Leipzig, Germany
- [c] Dr. N.K. Ojha, Prof. Dr. F. Zufall, Prof. Dr. T. Leinders-Zufall  
Center for Integrative Physiology and Molecular Medicine  
Saarland University  
Kirrbergerstraße 100, 66421 Homburg, Germany

**Abstract:** Photoswitchable reagents to modulate protein activity are powerful tools for high-spatiotemporal-precision control over endogenous biological functions. TRPC5 is a Ca<sup>2+</sup>-permeable cation channel with distinct tissue-specific roles, ranging from synaptic function to hormone regulation. Achieving spatially-resolved control over TRPC5 activity in particular cells or tissues, and temporal regulation in targeted cells, are therefore crucial milestones towards understanding and harnessing the biology of TRPC5. Here we develop the first photoswitchable TRPC5-modulating reagent, BTDAzo, towards reaching this goal. BTDAzo can photocontrol TRPC5 currents in cell culture, as well as controlling endogenous TRPC5-based neuronal Ca<sup>2+</sup> responses in mouse brain slices. BTDAzos are also the first reported azo-benzothiadiazines, an accessible and conveniently derivatised azoheteroarene that features excellent two-colour photoswitching. BTDAzo's TRPC5 control across relevant channel biology settings makes it appropriate for a range of dynamically reversible photoswitching studies in TRP channel biology, aiming to decipher the various biological roles of this centrally important ion channel.

## Introduction

The twenty-eight Transient Receptor Potential (TRP) channels have crucial roles in sensing and integrating a wide range of stimuli.<sup>[1]</sup> Better-known members include TRPV1 (heat) and TRPM8 (cold) for which a 2021 Nobel Prize was awarded, and TRPA1 (electrophiles). As these channels are expressed in many tissues but play different biological roles in these tissues,<sup>[2]</sup> potentially with time-dependent aspects, a range of photoswitchable ligands have been actively developed to elucidate their tissue- and time-specific roles through spatiotemporally precise modulation.<sup>[3]</sup> Notable photoswitchable TRP ligands include analogues of diacylglycerols (PhoDAGs)<sup>[4,5]</sup> and of small polar GSK ligands<sup>[6]</sup> for TRPC2,3,6; azo-vanilloids (azCA4<sup>[7]</sup>, red-azCA4<sup>[8]</sup>) for TRPV1; and TRPswitch<sup>[9]</sup> for TRPA1.

TRPC5 is implicated in a range of tissue-dependent roles in physiology as well as in disease, with brain functions from synaptic plasticity and hormone regulation to potential importance in metabolic medicine<sup>[2,10–12]</sup>. TRPC1,4 and 5 share substantial structural overlap which

drives the typically poor channel selectivity of TRPC1/4/5 ligands; however, drug discovery for TRPC5 has recently yielded a treasure trove of valuable ligands.<sup>[13,14]</sup> Weak antagonists were first identified from screening,<sup>[15]</sup> before it was identified by Waldmann as a target of the potent but nonselective TRPC4/5-targeting natural product agonist **Englerin A**<sup>[16,17]</sup> (**Fig. 1a**). Moderately potent synthetic agonist **BTD** was also identified by Schaefer, with the unusual feature of excellent selectivity for TRPC5 and no activity on TRPC4.<sup>[18]</sup> Boehringer-Hebra disclosed high-potency xanthine antagonist leads intended to treat anxiety,<sup>[19,20]</sup> that Bon and coworkers characterised as effective TRPC5 modulator tool compounds<sup>[21]</sup>; Bon developed these xanthines further to reach intriguing selectivity and mixed agonist-antagonist profiles (**AM237**; **Fig 1a**)<sup>[22]</sup> as well as identify the Pico145 binding site<sup>[23,24]</sup>.

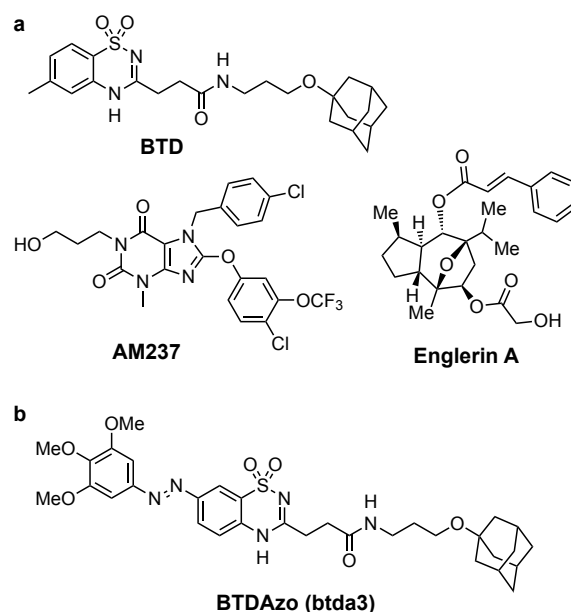


**Figure 1.** Design. (a) Known TRPC5 agonists **BTD**, **Englerin A**, **AM237**. (b) **BTDAzo**, the best photoswitchable agonist of the series **btdda1-7** (cf. **Fig S1**).

However, no photoswitchable TRPC5 ligands have yet been reported, which could help to study its tissue- and time-resolved biological roles. We therefore wished to

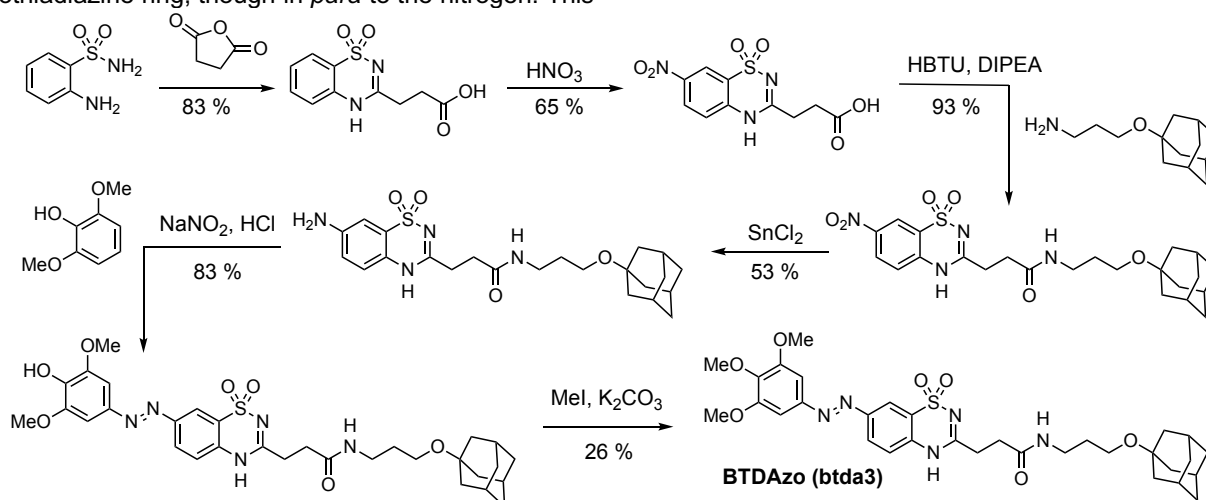
create TRPC5-selective photoswitchable ligands, with minimal effects on TRPC1/4 channels, as high spatiotemporal-precision tools with useful biochemical selectivity. **BTD** represented a good basis structure for this goal. Although its potency is moderate ( $EC_{50} \sim 1.4 \mu\text{M}$ ), it only activates homomeric TRPC5 or heteromeric TRPC[1/4]/5 channel complexes that contain TRPC5 subunits, making it a more selective tool than e.g. **AM237** or **Englerin A**. We set out to create a photoswitchable analogue of **BTD** for applications in researching the role of endogenous TRPC5 in mammalian cells and tissue slices.

## Results and Discussion

### Design and Synthesis

The TRPC5 binding mode of **BTD** is unknown, and structure-activity-relationship data are limited (the 4-methyl group on the benzothiadiazine can be deleted, but shorter spacers between the adamantane and benzothiadiazine abolish activity).<sup>[18]</sup> We tested applying the bidirectional photoswitch azobenzene to the **BTD** scaffold at each end, presuming that one end could be sterically tolerated.

Firstly, we extended the azobenzene from the benzothiadiazine ring, though in *para* to the nitrogen. This



**Scheme 1.** Synthesis of **BTDAzo** (**bt da3**).

### Photoswitchability

Pleasingly, the as-yet unstudied phenylazo-benzothiadiazine (**bt da1-4**) proved to be an excellent photoswitch, with performance recalling that of *para*-anilides. As expected for mono/*bis-para*-alkoxy azobenzenes,<sup>[26]</sup> **bt da5-7** also had high PSS ratios and efficient photoswitching. As **bt da3** later gave the best biological performance, it was renamed **BTDAzo**, and studied in detail. Like classical azobenzenes, the *E*-isomer is thermodynamically preferred, and all-*E* populations are reached by maintaining DMSO solution stocks at 60°C overnight. **BTDAzo** could be reversibly photoswitched between majority-*E* and majority-*Z* populations, reaching solvent-dependent PSSs with up to 94% *Z* (380 nm) and 87% *E* (520 nm) in apolar solvents that mimic the expected cellular lipid environment for this hydrophobic compound

was chosen hoping that this unknown azoheteroarene that is electronically similar to a *para*-anilide, could provide similarly desirable photoswitching properties, as are necessary for creating an effective photopharmaceutical: i.e. bidirectional photoswitching with near-UV and blue-green light each achieving high photostationary states (PSSs).<sup>[25]</sup> We varied the azophenyl substitution pattern to scan for different polarities, PSSs, and *Z*→*E* spontaneous relaxation rates: comparing unsubstituted, with *para*-methoxy and trimethoxy (improved PSSs), and *para*-hydroxy (faster relaxation) designs **bt da1-4** (**Fig S1**). Secondly, we replaced the hydrophobic adamantyl group with the azobenzene: retaining the oxyether attachment site because of its beneficial effects on photoswitching,<sup>[26]</sup> and employing an unsubstituted, *para*-methoxy, or a bulky adamantyl-mimicking bis-isopropyl azobenzene, in designs **bt da5-7** (**Fig S1**).

The seven candidates **bt da1-7** were assembled over three to six least linear steps, with good yields in all steps for except the final *O*-methylations of **bt da2-3**; representative synthesis of **bt da3** is shown in **Scheme 1**. **bt da1-7** were typically obtained in 10 mg batches and excellent purity, sufficient for biological evaluations (see **Supporting Information** for details).

(**Fig 2a-c**; **Fig S2**). The spectral separation between *E* and *Z* bands that results in the *Z* absorption minimum being located at the same wavelength as the *E* absorption maximum (**Fig 2d**) is the driver of the high-*Z* PSS.

Photoswitching in aqueous media was also excellently complete and was photoreversible over many cycles with no photoinstability noted (**Fig 2e**). *Z*→*E* thermal relaxation below 40°C was significantly slower than the timescales of channel switching experiments (**Fig S3**). PSS spectra and discussions of photochemistry for other **bt da** derivatives are given in the **Supporting Information** at **Fig S3-4**.

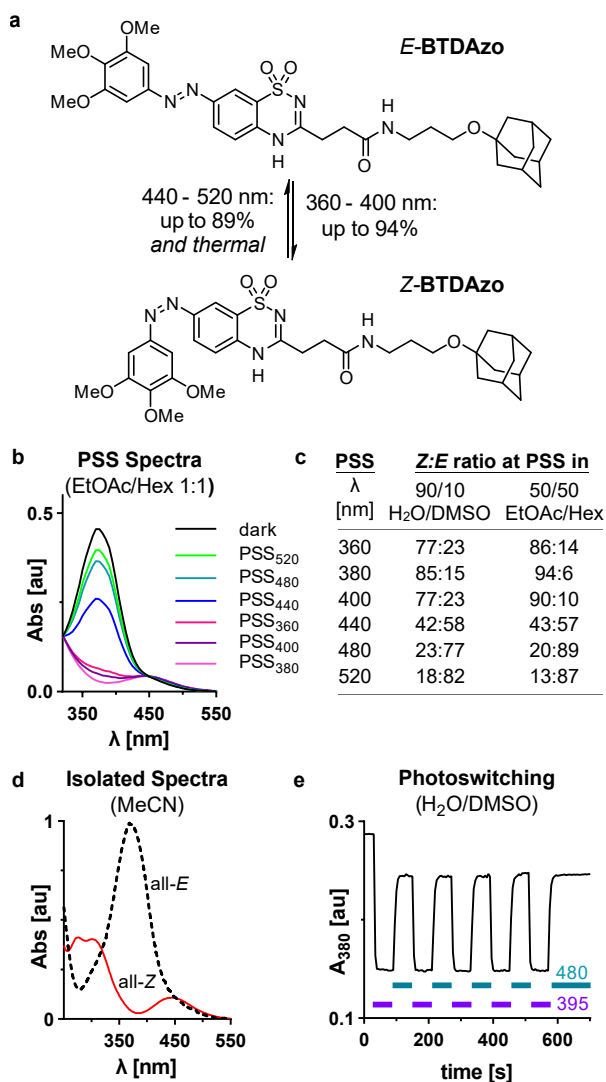


**Figure 2. Photocharacterisation.** (a)  $E \rightleftharpoons Z$  isomerisations of **BTDAzo**. (b)  $Z:E$  ratios at PSS depending on environment. (c) PSS spectra of **BTDAzo** in H<sub>2</sub>O/DMSO. (d) Spectra of pure  $E$ - and  $Z$ -**BTDAzo** (inline HPLC detection). (e) **BTDAzo** can be reversibly photoswitched between PSS states.

## Cellular TRPC5 Photopharmacology

We initially screened **btda1-7** as photoswitchable TRPC5 agonists in cells, using human embryonic kidney cell line HEK293 stably transfected to express a mouse TRPC5-CFP fusion protein (HEK<sub>m</sub>TRPC5-CFP). HEK<sub>m</sub>TRPC5-CFP cell suspensions were loaded with the fluorescent Ca<sup>2+</sup> indicator dye precursor Fluo-4/AM, washed, and dispensed into black pigmented clear-bottom 384-well microplates to monitor ion channel opening in a custom-made fluorescence imaging plate reader device. By adding serially diluted compounds to single wells, this is a convenient high-throughput method to obtain concentration-response curves before and during controlled application of ultraviolet light to the bottom of the microplate. We wished to use alternating cycles of moderate intensity 360/447 nm light for substantial  $E \rightleftharpoons Z$  photoswitching. The fluorescent Ca<sup>2+</sup> indicator Fluo-4 was

either excited at 447 nm for combined detection and off-switching, or at low intensities of 470-nm light to achieve a lower impact on **btda** photostationary states due to the small extinction coefficients in the cyan (**Fig S4**).

**BTDAzo (btda3)** was the best hit from this screening: it gave highly repeatable, bidirectional Ca<sup>2+</sup> influx signals with low basal activity as the relaxed  $E$  isomer and robust responses upon photoswitching with 365 nm light (**Fig 3a**). **BTDAzo** showed several outstanding features. Firstly, the potency of **Z-BTDAzo** (EC<sub>50</sub> 1.5  $\mu$ M, **Fig 3b**) was as good as that of its parent molecule **BTD** (EC<sub>50</sub> 1.4  $\mu$ M)<sup>[18]</sup>; potency matching is only very rarely achieved in photopharmacology.<sup>[27]</sup> Secondly, not only was all- $E$ -**BTDAzo** at 50  $\mu$ M fully inactive on TRPC5, and nearly non-responsive to 470 nm imaging (initial 60 s of **Fig 3a**), but photoswitching of 50  $\mu$ M mostly-**Z-BTDAzo** with 440 nm reduced channel currents to below those seen with mostly- $Z$  **BTDAzo** at just 1.5  $\mu$ M. It is **BTDAzo**'s combination of activity exclusively in the  $Z$ -isomer, with remarkably efficient  $Z \rightarrow E$  photoswitching at 440 nm in cells, that gives it such effective bidirectional *photoswitching of bioactivity*. Thirdly, no "biological fatigue" was seen, as photoswitching of was highly repeatable over many cycles. Thus **BTDAzo** could be a robust tool for complex studies (particularly since, as a lit-active photoswitch, it avoids background bioactivity in non-illuminated cells). The other **btidas** were not good tool compounds: **btda1,2,4** gave much slower bulk photoresponses, while **btda5-7** were inactive (see **Fig S5** and **Supporting Information**).

Since the plate imaging device uses single-color light-emitting diodes for Fluo-4 detection as well as for **BTDAzo** photoswitching, no continuous spectral information could be gathered in this assay. We therefore used single-cell Ca<sup>2+</sup> imaging with a Xenon lamp-equipped monochromator as excitation light source to study the cellular action spectra (channel current dependency on wavelength) and cellular power spectra (channel current dependency on applied photon flux), and to optimise assay illumination protocols.  $E \rightarrow Z$  action spectra showed optimal photo-switch-on response to ca. 360-370 nm (**Fig 3c-d**) when measured in flux-limited conditions designed to minimise photobleaching (power spectrum **Fig S6a-b**).  $Z \rightarrow E$  action spectra showed optimal photo-switch-off response to ca. 420-460 nm (**Fig 3e-f**) in flux-limited conditions (power spectrum **Fig S6c-d**). The striking action spectrum peak sharpness (**Fig 3d**), and the mismatch between the poor photoswitching completion in homogeneous polar media such as DMSO:water (**Fig 1c**) and the excellent performance in cells, indicate that cell-free measurements are only approximately predictive of the cellularly-relevant photoswitching of this lipophilic photoswitch (discussions in **Supporting Information** at **Fig S4** [relaxation timescales] and **Fig S6** [action spectra]). The power spectra additionally highlight that bulk  $E \rightarrow Z$  and  $Z \rightarrow E$  photoswitching in the cellular setting proceed at comparable rates (50% conversion at 30 mJ/cm<sup>2</sup> for 360 nm and 50 mJ/cm<sup>2</sup> for 440 nm; **Fig S6**); this is a reminder that the ratio of  $E/Z$  extinction coefficients is more important for photoswitching performance in microscopy, than are their absolute magnitudes (ca. tenfold lower at 440 nm than at 360 nm).

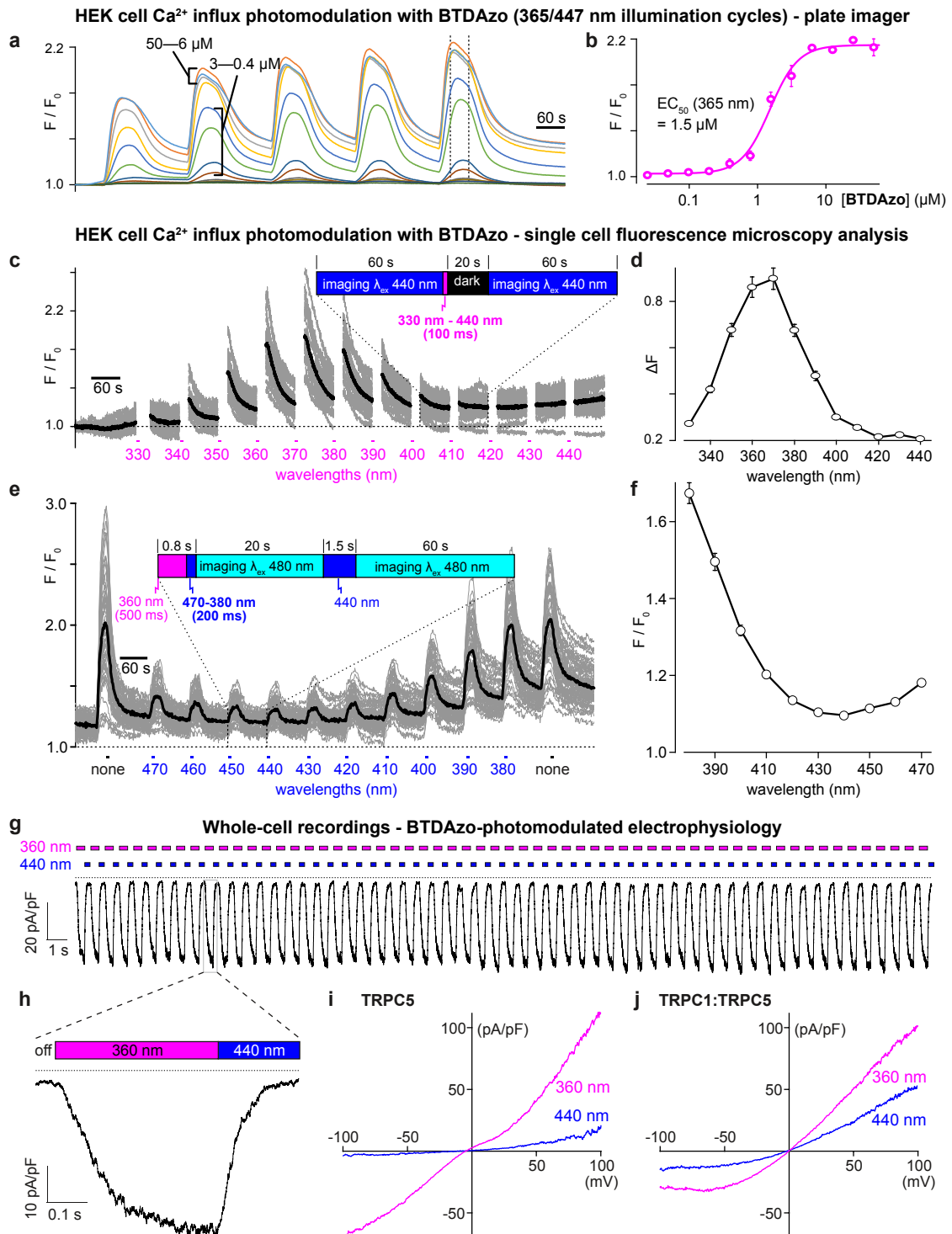


**Figure 3: Cellular TRPC5 photoswitching with BTDAzo.** (a-b) Reversible Ca<sup>2+</sup> influx modulation with BTDAzo under cycles of 365/447 nm illumination, and peak amplitudes (mostly Z-BTDAzo), as detected in Fluo-4-loaded HEK<sub>mTRPC5-CFP</sub> cell suspensions by fluorescence plate imager. (c-f) Microfluorometric single cell analysis (60 grey traces: single cells; black trace: averaged signal) of TRPC5 activation measured with a monochromator-equipped Xenon light source. (c-d) Cellular action spectrum for stimulation of Ca<sup>2+</sup> influx into single HEK<sub>mTRPC5-CFP</sub> cells by E→Z BTDAzo isomerisation. (e-f) Cellular action spectrum for shutdown of Ca<sup>2+</sup> influx (after E→Z isomerisation) by Z→E BTDAzo isomerisation at various wavelengths. (g-h) Electrophysiological whole-cell recordings of TRPC5 currents in voltage clamp (V<sub>h</sub> = -80 mV) mode. (g) Ionic currents in a TRPC5-expressing HEK293 cell during 60 consecutive cycles of 360/440 nm illumination in the presence of 10 μM BTDAzo. Dotted line: zero current level. (h) Magnification of a single on-off cycle taken from the trace shown in (g). (i) I/V curves of whole cell currents in a voltage-clamped TRPC5-expressing cell exposed to 360 nm and 440 nm light with 10 μM BTDAzo in the bath solution. (j) Patch-clamp traces obtained as in (i), but from a TRPC1/TRPC5-co-expressing cell. Note the distinct shape of the I/V curve with smaller inward current component.

We next performed patch clamp experiments, a non-optical current readout that can orthogonally confirm and characterise the specificity of channel modulation. In the

presence of 10 μM BTDAzo, on/off-photoswitching of ionic currents was fully reproducible over 60 cycles (Fig 3g) with 360 nm rapidly opening then 440 nm almost fully reclosing

channels to baseline conductivity (**Fig 3h**). The efficient channel closure following 440 nm illumination was seen over the entire current-voltage plot range (**Fig 3i**).

**BTD** is a strong tool compound because of its high selectivity for TRPC5-containing channels,<sup>[18]</sup> while most other TRPC5 ligands also target TRPC4. To test whether **BTD** retains this TRPC5-selectivity, we imaged TRPC4-expressing HEK293 cells in FLIPR, and pleasingly saw no TRPC4-mediated photostimulation of  $\text{Ca}^{2+}$  influx responses under any of the BTD derivatives applied at concentrations up to 50  $\mu\text{M}$ , including **BTD**Azo (**Fig S7**).

Patch clamp recordings in TRPC1/TRPC5 co-expressing cells exposed to 10  $\mu\text{M}$  **BTD**Azo, however, showed a strong photocontrol of inward and outward currents with a characteristic shape of the I/V curve known to result from the assembly of TRPC1 and TRPC5 channel subunits into heteromeric channel complexes (**Fig 3j**). This finding is reminiscent of the parent compound **BTD**, which also activates heteromeric TRPC1/C5 channel complexes.

Taken together, we conclude that **BTD**Azo is a selective, fully reversible "binary performance" photoswitchable agonist for cellular TRPC5.

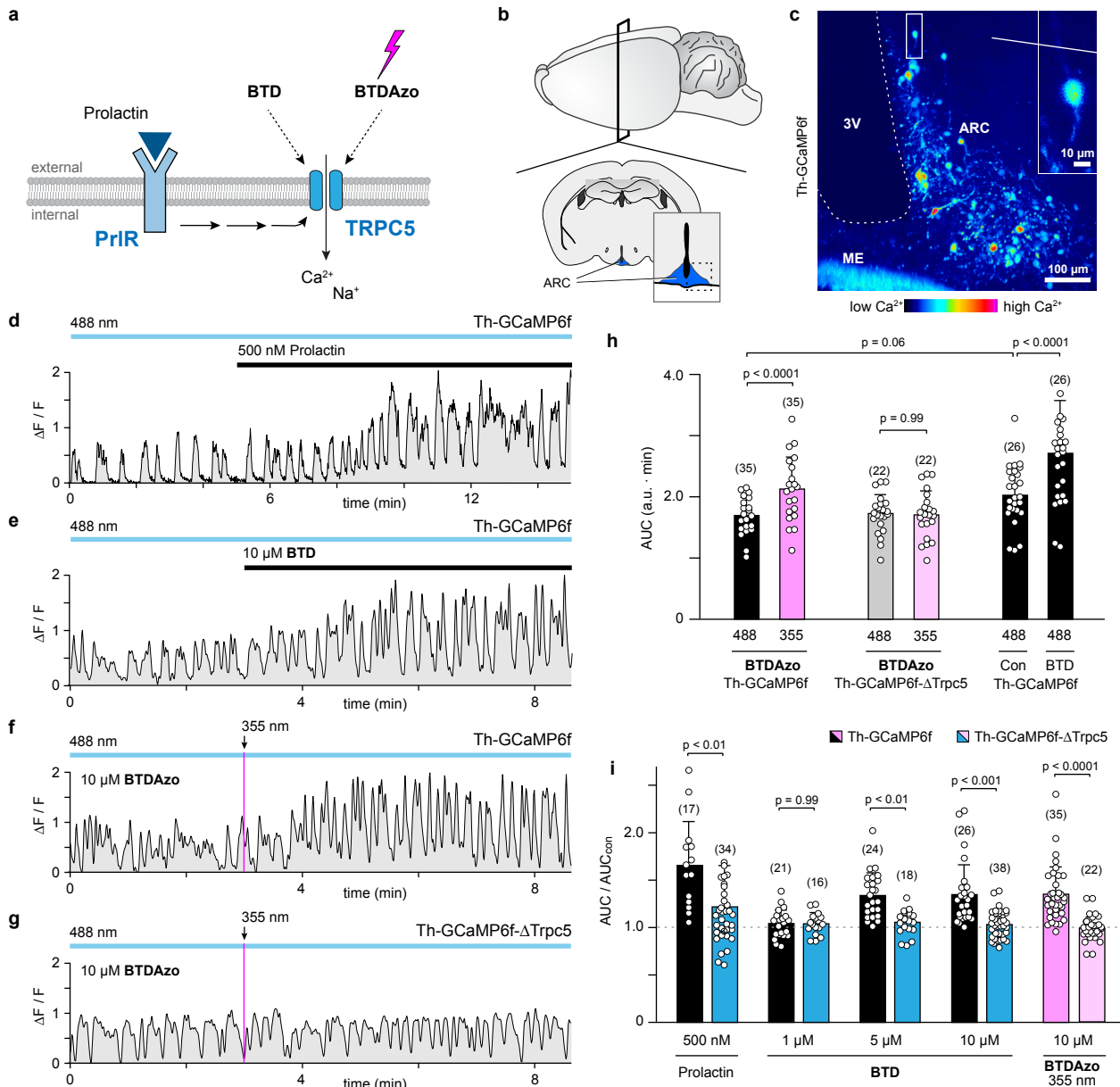


**Figure 4: BTD**Azo photocontrols endogenous TRPC5-dependent  $\text{Ca}^{2+}$  responses in mouse brain. (a) Cascade model for TRPC5-dependent cation channel activation in Th+ neurons of the hypothalamic arcuate nucleus (ARC) after stimulation of the prolactin receptor (PrIR). (b) Cartoon of the coronal brain slice, and region of the ARC (blue). Dashed box indicates the ARC region in (c). (c) Pseudocoloured image of Th+ neurons expressing GCaMP6f in a mouse brain slice. Inset: Zoom on a GCaMP6f neuron from the dorsomedial region of the ARC. (3V, third ventricle; ME, median eminence). (d-g) Original traces of spontaneous  $\text{Ca}^{2+}$  responses in Th+ neurons of Th-GCaMP6f mice, stimulated with prolactin (d), **BTD** (e), or **BTD**Azo followed by E $\rightarrow$ Z isomerisation using a 355 nm UV laser pulse (f-g). Panel (g) shows data for the TRPC5-deficient Th+ neuron of Th-GCaMP6f- $\Delta$ Trpc5 mouse. (h) Area under the curve (AUC) of  $\text{Ca}^{2+}$  signals when applying **BTD**Azo under 488 or 355 nm in wildtype or Trpc5 deficient Th+ neurons, compared with wildtype cosolvent only (Con) or **BTD** controls. Two-way ANOVA:  $F(3, 158) = 3.011$ ,  $p < 0.05$ . (i) Wildtype or knockout AUCs normalized to their controls (cosolvent or 488nm stimulation of **BTD**Azo) show prolactin, **BTD**, and **BTD**Azo after 355 nm photoswitching stimulate TRPC5-dependent  $\text{Ca}^{2+}$  increases. Kruskal-Wallis ANOVA:  $\chi^2(9) = 95.24$ ,  $p < 0.00001$ . [(h-i): number of cells is indicated in parentheses above each bar; for full description of material methods and statistics see **Supporting Information**.]

## Tissue slice photopharmacology – hypothalamic mouse dopamine neurons

We now wished to use **BTDAzo** to probe the role of TRPC5-dependent responses in dopamine (i.e. tyrosine hydroxylase-positive, Th+) neurons of the hypothalamic arcuate nucleus (ARC) (**Fig 4a**). TRPC5 contributes to both spontaneous oscillatory activity and persistent activation after stimulation with maternal signalling hormone prolactin, which is essential for normal prolactin homeostasis of the body (**Fig 4a**).<sup>[11]</sup>

We took slices through the ARC of mice expressing the Ca<sup>2+</sup> indicator GCaMP6f in Th+ neurons (**Fig 4b-c**) to test whether **BTDAzo** illumination could achieve photocontrol over Ca<sup>2+</sup> responses at endogenous TRPC5 expression levels. Spontaneous Ca<sup>2+</sup> responses in Th+ neurons after treatment with **BTDAzo** and 355 nm photoactivation matched those upon treatment with either prolactin or **BTD** (**Fig 4d-f**). Genetic deletion of the TRPC5 channel in the Th-GCaMP6f- $\Delta$ Trpc5 mouse prevented the increase in Ca<sup>2+</sup> activity in Th+ neurons (**Fig 4g**), indicating the channel selectivity of **BTDAzo** in the slice setting. The area under the curve (AUC) of the Ca<sup>2+</sup> signals quantifies that **BTDAzo** does not induce changes under 488 nm illumination alone, but needs both isomerisation with 355 nm light and TRPC5 expression to generate Ca<sup>2+</sup> rises ( $p < 0.0001$ ) (**Fig 4h-i**).

Thus, **BTDAzo** can be used in complex tissue slice settings as a highly selective direct activator of the TRPC5 channel complex that acts only upon  $E \rightarrow Z$  photoswitching to measurably increase sustained influxes of Ca<sup>2+</sup> mimicking those seen with the endogenous activator, prolactin.

## Conclusion

Photopharmaceuticals are proving to be powerful and flexible tools to non-invasively manipulate and study biological processes, with high temporal and spatial resolution that is appropriate to their function.<sup>[28,29]</sup>

We here report the first photoswitchable ligand for the ion channel TRPC5. **BTDAzo** can reversibly photoswitch cellular channel activity between opened (conducting) and full baseline states, and its potency and selectivity are additional promising features for future research. Its channel activation is potent enough to be applicable not only in overexpression systems, but in brain tissues with endogenous TRPC5 expression levels, and its pharmaceutical properties make it suitable for tissue slice use. Following the proof of concept brain slice assay we have tested, we consider **BTDAzo** as a valuable tool to investigate the various roles of TRPC5 (and TRPC4) in brain function, including their potential in the study and treatment of metabolic disease.<sup>[12]</sup>

We believe this is also the first report of azobenzothiadiazines as photoswitches for cell biology. It can give favourably complete bidirectional photoswitching with rapid response under biologically available wavelengths, and its easy synthesis and handling recommend it for use towards other photopharmaceuticals.

Challenges for the ongoing development and use of TRPC5 photopharmaceuticals in focus in our group include (i) improving ligand potency, and (ii) improving solubility and bioavailability, which should broaden the scope of applications of these ligands towards real-time *in vivo*

uses.<sup>[30]</sup> Nevertheless, **BTDAzo** is a reliable, potent TRPC5 photoswitch that can easily find applications in cell culture and slice use towards a better understanding of this truly remarkable protein.

## Acknowledgements

We thank the German Research Foundation (DFG: SFB TRR 152 number 239283807 projects P10 to FZ/TLZ, P18 to MS, P24 to OTS; Emmy Noether number 400324123 to OTS) for funding.

**Keywords:** TRPC5; photopharmacology; optical control; photoswitch; cation channel currents.

- [1] V. Flockerzi, B. Nilius, in *Mammalian Transient Receptor Potential (TRP) Cation Channels: Volume 1* (Eds.: B. Nilius, V. Flockerzi), Springer, Berlin, Heidelberg, **2014**, pp. 1–12.
- [2] S. Sharma, C. R. Hopkins, *J. Med. Chem.* **2019**, *62*, 7589–7602.
- [3] S. Curcic, O. Tiapko, K. Groschner, *Pharmacol. Ther.* **2019**, *200*, 13–26.
- [4] T. Leinders-Zufall, U. Storch, K. Blyemehl, M. Mederos y Schnitzler, J. A. Frank, D. B. Konrad, D. Trauner, T. Gudermann, F. Zufall, *Cell Chem. Biol.* **2018**, *25*, 215–223.e3.
- [5] T. Leinders-Zufall, U. Storch, M. Mederos y Schnitzler, N. K. Ojha, K. Koike, T. Gudermann, F. Zufall, *STAR Protocols* **2021**, *2*, 100527.
- [6] O. Tiapko, N. Shrestha, S. Lindinger, G. G. de la Cruz, A. Graziani, C. Klec, C. Butorac, W. F. Graier, H. Kubista, M. Freichel, L. Birnbaumer, C. Romanin, T. Glasnov, K. Groschner, *Chem. Sci.* **2019**, *10*, 2837–2842.
- [7] J. A. Frank, M. Moroni, R. Moshourab, M. Sumser, G. R. Lewin, D. Trauner, *Nat. Comm.* **2015**, *6*, 7118.
- [8] D. B. Konrad, J. A. Frank, D. Trauner, *Chem. Eur. J.* **2016**, *22*, 4364–4368.
- [9] P.-Y. Lam, A. R. Thawani, E. Balderas, A. J. P. White, D. Chaudhuri, M. J. Fuchter, R. T. Peterson, *J. Am. Chem. Soc.* **2020**, *142*, 17457–17468.
- [10] A. V. Zholos, in *Mammalian Transient Receptor Potential (TRP) Cation Channels* (Eds.: B. Nilius, V. Flockerzi), Springer Berlin Heidelberg, Berlin, Heidelberg, **2014**, pp. 129–156.
- [11] T. Blum, A. Moreno-Pérez, M. Pyrski, B. Bufe, A. Arifovic, P. Weissgerber, M. Freichel, F. Zufall, T. Leinders-Zufall, *PNAS* **2019**, *116*, 15236–15243.
- [12] R. S. Bon, D. J. Wright, D. J. Beech, P. Sukumar, *Annu. Rev. Pharmacol. Toxicol.* **2022**, *62*, 427–446.
- [13] A. Minard, C. C. Bauer, D. J. Wright, H. N. Rubaiy, K. Muraki, D. J. Beech, R. S. Bon, *Cells* **2018**, *7*, 52.
- [14] H. N. Rubaiy, *Br. J. Pharmacol.* **2019**, *176*, 832–846.
- [15] J. M. Richter, M. Schaefer, K. Hill, *Mol. Pharmacol.* **2014**, *86*, 514–521.
- [16] Y. Akbulut, H. J. Gaunt, K. Muraki, M. J. Ludlow, M. S. Amer, A. Bruns, N. S. Vasudev, L. Radtke, M. Willot, S. Hahn, T. Seitz, S. Ziegler, M. Christmann, D. J. Beech, H. Waldmann, *Angew. Chem. Int. Ed.* **2015**, *54*, 3787–3791.
- [17] M. J. Ludlow, H. J. Gaunt, H. N. Rubaiy, K. E. Musialowski, N. M. Blythe, N. S. Vasudev, K. Muraki, D. J. Beech, *J. Biol. Chem.* **2017**, *292*, 723–731.
- [18] H. Beckmann, J. Richter, K. Hill, N. Urban, H. Lemoine, M. Schaefer, *Cell Calcium* **2017**, *66*, 10–18.
- [19] S. Just, B. L. Chenard, A. Ceci, T. Strassmaier, J. A. Chong, N. T. Blair, R. J. Gallaschun, D. del Camino, S. Cantin, M. D'Amours, C. Eickmeier, C. M. Fanger, C. Hecker, D. P. Hessler, B. Hengerer, K. S. Kroker, S. Malekiani, R. Mihalek, J. McLaughlin, G. Rast, J. Witek, A. Sauer, C. R. Pryce, M. M. Moran, *PLOS ONE* **2018**, *13*, e0191225.
- [20] Bertrand L. Chenard, R. J. Gallaschun, *Substituted Xanthenes and Methods of Use Thereof*, **2014**, WO2014143799A3.
- [21] H. N. Rubaiy, M. J. Ludlow, M. Henrot, H. J. Gaunt, K. Miteva, S. Y. Cheung, Y. Tanahashi, N. Hamzah, K. E. Musialowski, N. M. Blythe, H. L. Appleby, M. A. Bailey, L. McKeown, R. Taylor, R. Foster, H. Waldmann, P. Nussbaumer, M. Christmann, R. S. Bon, K. Muraki, D. J. Beech, *J. Biol. Chem.* **2017**, *292*, 8158–8173.

- 
- [22] A. Minard, C. C. Bauer, E. Chuntharpursat-Bon, I. B. Pickles, D. J. Wright, M. J. Ludlow, M. P. Burnham, S. L. Warriner, D. J. Beech, K. Muraki, R. S. Bon, *Br. J. Pharmacol.* **2019**, *176*, 3924–3938.
- [23] D. J. Wright, K. J. Simmons, R. M. Johnson, D. J. Beech, S. P. Muench, R. S. Bon, *Commun. Biol.* **2020**, *3*, 1–11.
- [24] C. C. Bauer, A. Minard, I. B. Pickles, K. J. Simmons, E. Chuntharpursat-Bon, M. P. Burnham, N. Kapur, D. J. Beech, S. P. Muench, M. H. Wright, S. L. Warriner, R. S. Bon, *RSC Chem. Biol.* **2020**, *1*, 436–448.
- [25] V. A. Gutzeit, A. Acosta-Ruiz, H. Munguba, S. Häfner, A. Landra-Willm, B. Mathes, J. Mony, D. Yarotski, K. Börjesson, C. Liston, G. Sandoz, J. Levitz, J. Broichhagen, *Cell Chem. Biol.* **2021**, *28*, 1648-1663.e16.
- [26] M. Borowiak, W. Nahaboo, M. Reynders, K. Nekolla, P. Jalinot, J. Hasserodt, M. Rehberg, M. Delattre, S. Zahler, A. Vollmar, D. Trauner, O. Thorn-Seshold, *Cell* **2015**, *162*, 403–411.
- [27] O. Thorn-Seshold, J. Meiring, *ChemRxiv* **2021**, DOI 10.26434/chemrxiv.14424176.v1.
- [28] J. Broichhagen, J. A. Frank, D. Trauner, *Acc. Chem. Res.* **2015**, *48*, 1947–1960.
- [29] M. J. Fuchter, *J. Med. Chem.* **2020**, *63*, 11436–11447.
- [30] X. Gómez-Santacana, S. Pittolo, X. Rovira, M. Lopez, C. Zussy, J. A. R. Dalton, A. Faucherre, C. Jopling, J.-P. Pin, F. Ciruela, C. Goudet, J. Giraldo, P. Gorostiza, A. Llebaria, *ACS Cent. Sci.* **2017**, *3*, 81–91.